ISSN: 2472-3703 DOI: 10.6911/WSRJ.202602_12(2).0008

Structural Design and Dynamic Sealing Failure Optimization of Metal C-Rings

Xiaojiang Li, Li Li, Jiaoshan Hao, Yan Feng

Chongqing Chuanyi Control Calve Co., Ltd., China

Abstract

Targeting the miniaturized static sealing and control valve radial dynamic sealing conditions, this paper constructs an integrated "Design-Verification-Optimization" research framework for metal C-rings. Based on the Inconel X750/718/Ag multilayer composite structure, high-temperature and high-pressure static sealing tests and reciprocating dynamic sealing wear studies were conducted. The results indicate that the helium leak rate of this C-ring at room temperature reaches 6.6×10^{-9} Pa• m^3/s, and it passed the verification of 21.5 MPa water pressure and 40 high-temperature cycles. Dynamic sealing failure is dominated by friction and wear; when the sleeve bore roughness is reduced to Ra=0.8 μm, the life is significantly extended to over 15,000 cycles, with limited benefits from further reducing roughness. Considering both cost and performance, it is recommended to set the roughness threshold for both the dynamic sealing mating surface and the static sealing surface at Ra≈0.8 μm.

Keywords

Metal C-ring seal; control valve; High temperature and high pressure; Radial dynamic sealing; Friction and wear; Surface roughness optimization.

1. INTRODUCTION

1.1. Research Background

Control valves are widely used in the petrochemical, high-temperature power, pharmaceutical, food, metallurgical and water treatment industries. As key components for controlling the direction and flow rate of fluids, the sealing performance of their critical parts directly determines the economy and safety of the entire system. With the development of control valves towards automation and integration, the design requirements for precision control valves are becoming increasingly urgent. Within such limited spaces, traditional non-metal sealing gaskets are constrained by factors such as friction and high-temperature creep, making it difficult for them to meet long-life service requirements. In contrast, metal seals (especially metal C-rings) are widely used in vacuum/high-pressure devices due to their reliability and environmental adaptability; their sealing mechanism, which establishes an interface barrier through elastic rebound and contact stress, provides more controllable leakage risks under extreme conditions. particularly under severe operating conditions with operating temperatures up to 345°C and pressures up to 14.5 MPa, metal C-rings must not only maintain extremely low leakage in a static state but also undertake radial reciprocating dynamic sealing functions in key components such as control valves. At this time, the sealing interface is governed by both roughness and real contact area during the coupled evolution of load-contact-microchannels, thereby posing dual challenges to structural design and tribological performance.

ISSN: 2472-3703 DOI: 10.6911/WSRJ.202602_12(2).0008

1.2. Research Status

Regarding the performance of metal C-ring seals, current academic and industrial research mainly focuses on two dimensions: static sealing mechanisms and dynamic friction and wear. In terms of static sealing, research generally revolves around the improvement of geometric structure and rebound/energy storage capabilities, verifying contact stress distribution and elastic energy storage characteristics under different compression depths through finite element simulation and experiments. Simultaneously, reliability assessments oriented towards engineering applications are also used to support design verification and test platform validation. Additionally, to improve long-term stability in extreme environments, research on stress relaxation and precipitate evolution of high-temperature elastic/load-bearing materials (such as Inconel X750/718) provides a materials science basis for the long-term rebound decay mechanism of sealing elements.

In terms of dynamic sealing, research focuses on tribological behavior and leakage channel evolution during reciprocating sliding: metal-to-metal sealing surfaces typically possess turned grooves and multi-scale roughness features, with leakage controlled jointly by "macroscopic topography (waviness/grooves) and microscopic roughness". From the perspective of mechanism modeling, rough surface contact can be characterized using statistical contact theory to describe real contact area and gap distribution, and further establish leakage rate prediction frameworks through percolation/effective medium concepts [10-11]. From the perspective of fluid lubrication, the average flow model provides a classical descriptive tool for the coupling of flow and load bearing between rough surfaces. Engineering practice also indicates that manufacturing surface quality (especially roughness) has a decisive impact on sealing performance: the higher the roughness, the easier it is for interface microchannels to connect, leading to increased leakage. Therefore, super-finishing of mating parts and surface consistency control are regarded as general strategies for life extension.

1.3. Existing Problems

Although independent research on static and dynamic sealing has yielded rich results, there are still significant limitations in engineering applications for automatic control valve, mainly reflected in two problems: "design segregation" and "lack of criteria." First, existing research often treats the structural strength design of static seals and the surface wear control of dynamic seals separately: static sealing research usually focuses on compression rebound and contact stress, while dynamic sealing research pays more attention to the influence of sealing surface topography on leakage and wear. Without a unified framework, the degradation of contact status caused by long-term fretting wear is difficult to incorporate into the design closed-loop of static sealing. Second, in the manufacturing process control of radial dynamic seals, there is a lack of reusable quantitative roughness acceptance standards: although "smoother is generally better for sealing" can be explained by the roughness-leakage rate relationship, determining the threshold at which performance improvement shows diminishing returns requires establishing executable criteria by combining leakage models [10-11] with engineering test data. Third, dynamic sealing life is also affected by wear mechanisms such as adhesion/abrasion [15, 16], and the topography evolution caused by wear will in turn change the connectivity of leakage channels, meaning the "roughness-wear-leakage" coupling effect has not yet been fully quantified in existing research.

In view of this, this paper aims to construct an integrated research framework connecting "structural design—simulation verification—static sealing validation—dynamic sealing failure analysis." Under unified engineering constraints, it systematically verifies the static sealing limit performance of miniaturized C-rings and focuses on quantifying the influence law of mating surface roughness on dynamic sealing life, thereby providing reusable theoretical bases and data support for the design optimization and manufacturing acceptance of sealing structures.

ISSN: 2472-3703 DOI: 10.6911/WSRJ.202602_12(2).0008

2. RESEARCH FRAMEWORK AND TECHNICAL ROUTE

This paper constructs a closed-loop research framework of "theoretical design—simulation verification—experimental validation—mechanism optimization," aiming to connect the technical link between static sealing verification and dynamic sealing life extension. It mainly includes the following core links:

Condition Definition and Structural Design: Based on 345°C/14.5 MPa operating conditions, design the Inconel X750/718 and silver layer composite C-ring structure. Use FEA simulation to verify rebound and contact characteristics, optimizing geometric parameters to avoid design risks.

Static Sealing Performance Verification: Establish a multi-physics test system to establish the sealing performance baseline under extreme environments and verify structural integrity through helium mass spectrometry leak detection, high-temperature stress relaxation, 21.5 MPa water pressure, and long-period high-temperature cycle testing.

Failure Analysis and Parameter Optimization: Targeting radial dynamic sealing, conduct 1,500 reciprocating wear tests and microscopic characterization (metallography/EDS) to reveal the "plowing-oxidation-abrasion" failure mechanism. Through sleeve roughness gradient comparison (Ra 3.2~0.4 μm), identify the performance inflection point for life enhancement and the optimal threshold.

Criteria Construction and Application: Based on test data, establish the mapping relationship between roughness and life, output manufacturing acceptance criteria that balance cost and reliability, and form reusable engineering specifications.

The research framework of this paper is shown in the flowchart below:

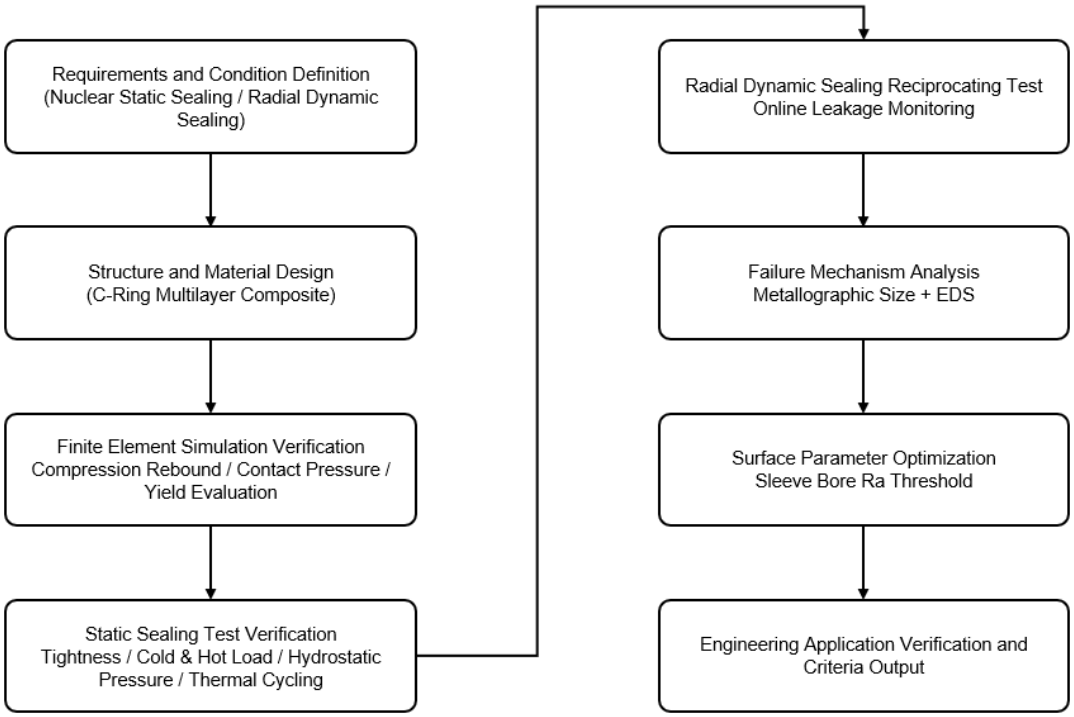


Figure 1. 'Design-Verification-Optimization' Integrated Research Framework

ISSN: 2472-3703 DOI: 10.6911/WSRJ.202602_12(2).0008

3. DESIGN OF C-RING AND STATIC SEALING PERFORMANCE VERIFICATION

3.1. Conditions and Structural Constraints

Key environmental parameters: Operating pressure atmospheric/14.5 MPa; maximum operating temperature 345°C; medium is water; design life 10 years; hydrostatic test pressure 21.4 MPa (room temperature).

3.2. Structure and Materials

Structural Design: The sealing structure is a compact flange, selecting a miniaturized C-ring matched with a narrow sealing groove. Seal ring dimensions (D×d)=ϕ37.9×ϕ3.2 mm, sealing groove dimensions ϕ38.2×4.1×2.6 mm; bolt specification is M8, installation torque 7.8 N·m, allowable torque 13.5 N·m.

Material System: The spring material is solution-treated Inconel X750, the intermediate layer is solution-treated Inconel 718 (referencing AMS 5596K), and the outer layer is pure silver (≥99.99%); critical surface roughness requirement is Ra≤0.8 μm.

3.3. Simulation Analysis Points

A periodic symmetric 3D solid model was adopted, with appropriate simplifications made for the silver layer in force calculations. At a total compression of 0.6 mm, the maximum equivalent stress is approximately 3039.7 MPa, exceeding the Inconel X750 yield strength of 1223 MPa. This indicates that the spring section is in a significant yield energy absorption state, and rebound and contact pressure stability should be evaluated under an elastic-plastic framework (as shown in Figure 2).

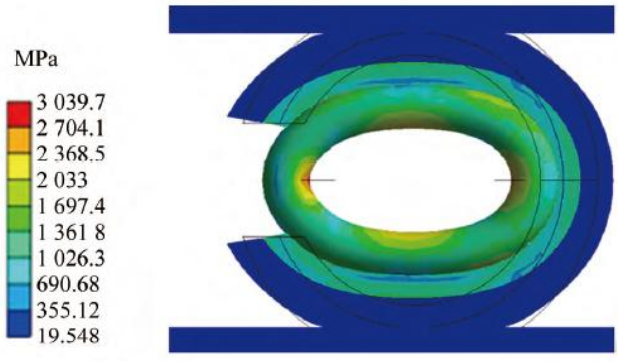


Figure 2. Equivalent stress distribution of C-ring under compression

3.4. Static Sealing Test Results

Tightness: Under room temperature and 0.1 MPa pressure difference, the helium leak rate is 6.6×10^{-9} Pa·m^3/s. Cold and hot state load-displacement results show that full sealing can be achieved when compressed to the design thickness, with the leak rate stabilizing at 3.0×10^{-9} Pa·m^3/s and a linear sealing load of about 328 N/mm (as shown in Figure 3).

ISSN: 2472-3703 DOI: 10.6911/WSRJ.202602_12(2).0008

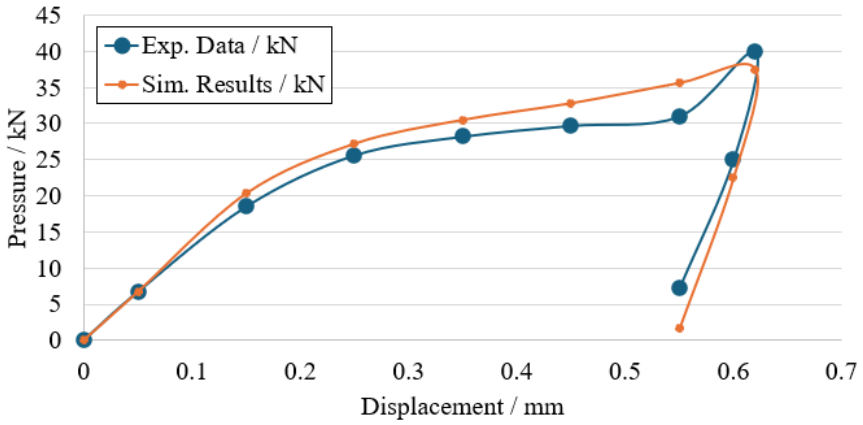


Figure 3. Exp. and Sim. Results for Compression-Rebound Characteristics

Figure 3: Comparison of Experimental and Simulation Results for Compression-Rebound Characteristics

Stress Relaxation: Under room temperature and 345°C conditions, the 4-hour relaxation rates were 1.96% and 2.09%, respectively. After the test, the sealing ring showed no crushing, peeling, or shedding of the sealing layer.

Water Pressure and high-temperature Cycles: Pressure was increased in stages to 21.5 MPa at room temperature and held for ≥30 min; no visible leakage or pressure drop occurred. A total of 40 high-temperature cycles (working temperature ≥345°C, holding time ≥15 min, heating/cooling rate ≥80°C/h) were conducted, with no abnormalities such as leakage or silver layer detachment observed.

4. FAILURE MECHANISM AND ROUGHNESS PARAMETER OPTIMIZATION UNDER RADIAL DYNAMIC SEALING CONDITIONS

4.1. Reciprocating Test Scheme

A C-ring/sleeve bore reciprocating motion test was conducted under a 5% radial elastic deformation rate: stroke 8 mm, frequency 0.3 Hz, velocity 10 mm/s; sealing chamber helium pressure 0.8 MPa; 15,000 cycles. Failure was defined as a leak rate $>1\times10^{-6}$ Pa·m^3/s.

4.2. Samples and Roughness Gradient

To comprehensively reveal the non-linear influence of mating surface topography on the sealing interface, the experiment designed four groups of gradient samples (S1~S4) covering typical engineering machining precisions. As shown in the table, sample preparation spanned the complete processing chain from "rough turning" to "super-fine polishing". Among them, the S1 group (Ra≈3.2 μm) retained significant periodic turning tool marks, simulating conditions with poorly controlled machining quality; the S2 group eliminated macroscopic tool marks through coarse grinding but still retained random grinding marks; the S3 and S4 groups further reduced surface roughness to the sub-micron level (Ra≤0.8 μm) through fine grinding and polishing processes, presenting dense mirror-like features. This gradient setting not only reproduces various surface qualities encountered in engineering but, more critically, achieves the evolution of surface micro-topography from "deterministic peaks and valleys" to "stochastic micro-asperities," providing a clear physical baseline for subsequently separating the coupled mechanisms of mechanical wear and oxidative wear.

ISSN: 2472-3703 DOI: 10.6911/WSRJ.202602_12(2).0008

Table 1. Test Sample Grouping, Processing Technology, and Surface State Description

Group	Ra / μm	Processing Technology	Surface State
S1	3.2±0.2	Normal turning (60m/min, 0.2mm/r)	Visible turning marks, local burrs
S2	1.6±0.1	Fine turning (80m/min) + Wheel coarse grinding (800#)	Turning marks eliminated, slightly rough
S3	0.8±0.08	Fine turning (100m/min) + Wheel fine grinding (1200#) + Polishing	Smooth without scratches, delicate feel
S4	0.4±0.05	Fine turning + Wheel fine grinding (2000#) + Super-fine polishing	Mirror effect, extremely fine processing traces

4.3. Evolution of Leakage with Number of Cycles

The changes in leakage under different roughness levels are shown in the table below. The greater the roughness, the faster the leakage growth and the earlier the failure criterion is reached; when Ra is reduced to 0.8 μm, the difference from the 0.4 μm group tends to be insignificant (as shown in Figure 4).

Table 2. Evolution of Leakage Under Different Roughness Levels Leakage ($\times 10^{-7}$ Pa·m^3/s)

Cycle Count (Cycles)	S1 (Ra=3.2μm)	S2 (Ra=1.6μm)	S3 (Ra=0.8μm)	S4 (Ra=0.4μm)
Initial	0.32	0.28	0.25	0.26
3000	5.80	2.10	0.95	0.92
6000	15.00 (Failed)	6.50	1.80	1.75
9000	— (Failed)	11.00 (Failed)	3.20	3.10
15000	— (Failed)	— (Failed)	8.20	7.80

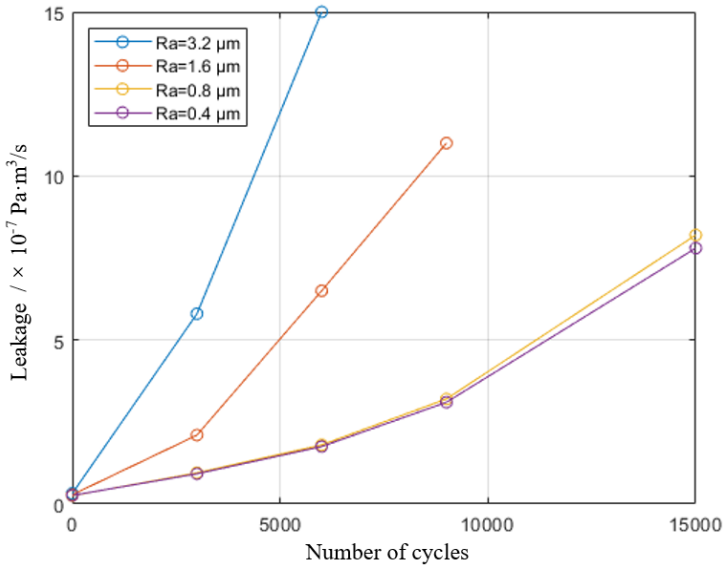


Figure 4. Evolution Curves of Leak Rate with Cycle Count Under Different Roughness Levels

4.4. Metallographic Size Quantification and Failure Stage Division

Metallographic results show: High roughness groups exhibit deeper plow grooves and a higher proportion of material spalling area, while the oxide layer is more prone to fracture; combined with EDS, a significant increase in O element is visible in the wear zone accompanied

ISSN: 2472-3703 DOI: 10.6911/WSRJ.202602_12(2).0008

by transfer of mating part elements, indicating a coupled mechanism of wear-oxidation-abrasion.

Table 3. Microscopic Wear Indicators and Oxidation State

Observation Item	S1 (Failed)	S2 (Failed)	S3 (15000 Cycles)	Detection Method
Plow groove depth (μm)	8.2±1.5	4.1±0.8	0.9±0.2	500x Microscope Crosshair Measurement (n=10)
Material spalling area ratio (%)	21.3±3.1	7.8±1.5	0.5±0.2	2000x Microscope Image Analysis
Oxide layer state	Fracture (Thickness 0.6μm)	Local fracture (Thickness 0.8μm)	Continuous dense (Thickness 0.8μm)	EDS Energy Spectrum Line Scan

Based on this, the failure process can be divided into: ① Mechanical Wear Stage (Peak/valley plowing destroys the surface layer); ② Oxidative Wear Stage (Oxide layer generation - fracture forms abrasive particles); ③ Sealing Failure Stage (Gap enlargement and contact area reduction lead to a sudden increase in leakage).

5. CONCLUSION

Proposed and verified a C-ring static sealing scheme for control valve. This paper constructed a miniaturized structure and assembly window for a multi-layer composite metal C-ring (Inconel X750/718 + Ag coating). In the multi-indicator sequence verification of "leak detection—pressure bearing—high-temperature cycling," results showed: under room temperature and 0.1 MPa pressure difference, the helium leak rate reached 6.6×10^{-9} Pa·m^3/s, and stable full sealing was achieved when compressed to the design thickness (leak rate approx. 3.0×10^{-9} Pa·m^3/s). Furthermore, after maintaining pressure at 21.5 MPa and undergoing 40 high-temperature cycles, the sealing interface showed no signs of abnormal failure, proving that this miniaturized scheme possesses engineering reliability under high-temperature and high-pressure operating conditions.

Revealed the dominant mechanism and staged evolution laws of C-ring failure under radial dynamic sealing conditions. Under conditions of 5% radial elastic deformation rate, 0.8 MPa sealing chamber pressure, and reciprocating cyclic loading, combined with leakage evolution and metallographic/energy spectrum evidence, this paper confirmed that failure is controlled by friction and wear. It presents a stage chain of "mechanical plowing destroys surface layer — oxide layer generation/fracture forms abrasive particles—effective contact area attenuation leads to sudden leakage increase," providing an explainable mechanistic basis for dynamic sealing life prediction and process control.

Provided quantitative thresholds and engineering criteria for dynamic sealing mating surface roughness. Based on roughness gradient comparison tests, this paper showed that mating surface roughness has a significant control effect on leakage growth and life: at Ra=3.2 μm and 1.6 μm, the failure criteria were reached at approximately 6,000 and 9,000 cycles respectively. However, when Ra≈0.8 μm (and lower), the seal remained unfailed within 15,000 cycles, and leakage growth was significantly controlled. Considering the diminishing returns of performance improvement and processing costs, it is recommended to control the roughness of the radial dynamic sealing mating sleeve bore at Ra≈0.8 μm as the preferred threshold to form a reusable process control criterion.

ISSN: 2472-3703 DOI: 10.6911/WSRJ.202602_12(2).0008

REFERENCES

[1] Zhou Y Q, Feng H S, Zhuang M, et al. Reliability assessment of metal C-ring sealing performance for CFETR torus cryopump main valve[J]. Vacuum, 2025, 233: 113930. doi:10.1016/j.vacuum.2024.113930.

[2] Kim G H, Her N I, Kim H T. A design study on metal C-ring seals [J]. Vacuum, 2022, 205: 111401. doi:10.1016/j.vacuum.2022.111401.

[3] Kim G H, Lee Y S, Yang H L. Experimental verification of newly proposed design of metal O-ring seal [J]. Vacuum, 2021, 184: 109942. Doi: 10.1016/j.vacuum.2020.109942.

[4] Wang Y, Luo W, Liu S, et al. A model for reliability assessment of sealing performance of the C-shaped metal sealing ring at the outlet of the subsea tubing hanger [J]. Ocean Engineering, 2022, 243: 110311. Doi: 10.1016/j.oceaneng.2021.110311.

[5] Ha J W, Seong B S, Jeong H W, et al. Effects of the aging temperature and stress relaxation conditions on γ' precipitation in Inconel X-750 [J]. Journal of Nuclear Materials, 2015, 457: 362-368. doi:10.1016/j.jnucmat.2014.11.093.

[6] Wang Y, Zhang X, et al. A parametric study and experimental validation of all-metal angle valve seals with different surface roughness and coatings [J]. Processes, 2025, 13(4): 968.

[7] Gao B, et al. On the sealing mechanism and performance of self-tightening B-ring seal [J]. Processes, 2022, 10: 1084.

[8] Cheng H, et al. Structural parameter effects and finite element evaluation for combined metal sealing ring [J]. Applied Sciences, 2022, 12: 714.

[9] Roth A. The influence of the surface roughness on the specific leak rate of gasket seals [J]. Vacuum, 1970, 20(10): 431-435. doi:10.1016/S0042-207X(70)80056-2.

[10] Persson B N J, Yang C. Theory of the leak-rate of seals [J]. Journal of Physics: Condensed Matter, 2008, 20(31): 315011. doi:10.1088/0953-8984/20/31/315011.

[11] Lorenz B, Persson B N J. Leak rate of seals: Effective-medium theory and comparison with experiment [J]. Eur Phys J E Soft Matter, 2010, 31(2): 159-167. doi:10.1140/epje/i2010-10558-6.

[12] Pérez-Ràfols F, Larsson R, Almqvist A. Modelling of leakage on metal-to-metal seals [J]. Tribology International, 2016, 94: 421-427. doi:10.1016/j.triboint.2015.10.003.

[13] Patir N, Cheng H S. An average flow model for determining effects of three-dimensional roughness on partial hydrodynamic lubrication [J]. ASME Journal of Lubrication Technology, 1978, 100(1): 12-17. doi: 10.1115/1.3453103.

[14] Greenwood J A, Williamson J B P. Contact of nominally flat surfaces [J]. Proceedings of the Royal Society of London. Series A, Mathematical and Physical Sciences, 1966, 295(1442): 300-319. doi: 10.1098/rspa.1966.0242.

[15] Archard J F. Contact and rubbing of flat surfaces [J]. Journal of Applied Physics, 1953, 24(8): 981-988. doi: 10.1063/1.1721448.

[16] Liu Qiang, Liu Ke, Tu Shenghui. Design and Sealing Performance of Miniaturized C-Ring for Nuclear Grade Equipment [J]. Mechanical Design and Research, 2025(3):355-358. doi:10.13952/j.cnki.jofmdr.2025.0229